

having a very small size effect such as an Au-Ag disordered alloy.

The authors thank Mr M. Minoura and Mr K. Ushida for their help. They also express their sincere thanks to Dr Y. Amemiya of the Photon Factory, National Laboratory for High Energy Physics. They are indebted to Dr S. C. Moss, University of Houston, for a critical reading of the manuscript.

#### References

- AMEMIYA, Y., MATSUSHITA, T., NAKAGAWA, A., SATOW, Y. & MIYAHARA, J. (1988). *Nucl. Instrum. Methods*, **A266**, 645-653.  
 BUSHUEV, V. A., LAUSHKIN, A. V., KUZ'MIN, R. N. & LOBANOV, N. N. (1983). *Sov. Phys. Solid State*, **25**, 228-233.  
 BUSHUEV, V. A. & LYUBIMOV, A. G. (1987). *Sov. Phys. Crystallogr.* **32**, 179-184.

- CAIN, L. S. & THOMAS, J. F. JR (1971). *Phys. Rev. B*, **4**, 4245-4255.  
 CHOU, H., SHAPIRO, S. M., MOSS, S. C. & MOSTOLLER, M. (1990). Submitted to *Phys. Rev. B*.  
 EPPERSON, J. E., FÜRNRÖHR, P. & ORTIZ, C. (1978). *Acta Cryst.* **A34**, 667-681.  
 HAMILTON, W. C. (1957). *Acta Cryst.* **10**, 629-634.  
 KAINUMA, Y. (1955). *Acta Cryst.* **8**, 247-257.  
 KAINUMA, Y. (1961). *J. Phys. Soc. Jpn*, **16**, 228-241.  
 KASHIWASE, Y., KAINUMA, Y. & MINOURA, M. (1981). *J. Phys. Soc. Jpn*, **50**, 2793-2794.  
 KASHIWASE, Y., KAINUMA, Y. & MINOURA, M. (1982). *Acta Cryst.* **A38**, 390-391.  
 KASHIWASE, Y., MORI, M., KOGISO, M., MINOURA, M. & SASAKI, S. (1988). *J. Phys. Soc. Jpn*, **57**, 524-534.  
 KASHIWASE, Y., MORI, M., KOGISO, M., USHIDA, K., MINOURA, M., ISHIKAWA, T. & SASAKI, S. (1989). *Phys. Rev. Lett.* **62**, 925-928.  
 OYA, Y. & KASHIWASE, Y. (1988). *J. Phys. Soc. Jpn*, **57**, 2026-2039.  
 WARREN, B. E. (1969). *X-ray Diffraction*, Ch. 12. Reading, MA: Addison-Wesley.  
 ZACHARIASEN, W. H. (1967). *Acta Cryst.* **23**, 558-564.

*Acta Cryst.* (1990). **A46**, 929-934

### Direct Methods in Superspace.

## II. The First Application to an Unknown Incommensurate Modulated Structure\*

BY XIANG SHI-BIN, FAN HAI-FU,† WU XIAO-JING AND LI FANG-HUA

*Institute of Physics, Chinese Academy of Sciences, Beijing 100080, People's Republic of China*

AND PAN QING

*Structure Research Laboratory, University of Science and Technology of China, Hefei 230026, People's Republic of China*

(Received 16 February 1990; accepted 28 June 1990)

#### Abstract

The direct method previously proposed [Hao, Liu & Fan (1987). *Acta Cryst.* **A43**, 820-824] has been used to determine the incommensurate modulation in the structure of ankangite by using the  $h0l$  electron diffraction pattern. Ankangite is a newly discovered mineral which belongs to the priderite group with chemical composition  $\text{Ba}_{0.8}(\text{Ti}, \text{V}, \text{Cr})_8\text{O}_{16}$ . The  $h0l$  electron diffraction pattern shows sharp satellite reflections which correspond to a one-dimensional incommensurate modulation along the  $c$  axis. Direct phasing of the  $h0l$  satellite reflections based on the known phases of the main reflections led to a three-dimensional hyperprojection along the  $a_2$  direction of the four-dimensional electron potential distribution, revealing clearly occupational and positional

modulations of the Ba atoms. Positional modulation of other atoms has also been observed.

#### Introduction

The purpose of the present study is threefold:

(1) Ankangite  $\text{Ba}_{0.8}(\text{Ti}, \text{V}, \text{Cr})_8\text{O}_{16}$  is a newly found mineral belonging to the priderite group (Xong, Ma & Peng, 1984). Electron-microscopy studies found that the mineral is an incommensurate modulated phase. A prediction for the form of modulation has also been made qualitatively based on electron diffraction patterns and high-resolution electron micrographs (Wu, Li & Hashimoto, 1990). A quantitative determination of the incommensurate modulation is useful for better understanding of the structure.

(2) Recently, a direct method has been proposed for solving incommensurate modulated structures (Hao, Liu & Fan, 1987, hereafter referred to as paper I). Unlike the others, this method does not rely on any assumption about the property of modulation. It

\* Supported by the National Natural Science Foundation of China.

† To whom all correspondence should be addressed.

solves the phase problem of the satellite reflections directly and reveals the modulation objectively. However, up to the present, the method has only been tested with a known structure. It needs to be tested further by solving unknown structures. Ankangite is a good sample for this purpose.

(3) Although direct methods are widely used in X-ray crystallography, they are seldom used in electron diffraction analysis. The present study gives a practical example of solving an incommensurate modulated structure by direct-method electron-diffraction analysis.

### Experiment

The mineral specimen was crushed into fine particles in an agate mortar and then put onto a holey carbon film supported by a copper mesh. The electron diffraction patterns were taken with a JEM-200CX electron microscope operated at an accelerating voltage of 200 kV. The Laue symmetry is found to be  $4/m$ . The main as well as the satellite reflections can be indexed using a four-dimensional reciprocal unit cell defined by  $\mathbf{b}_1$ ,  $\mathbf{b}_2$ ,  $\mathbf{b}_3$  and  $\mathbf{b}_4$ . For the four-dimensional representation of an incommensurate modulated structure, the reader is referred to the paper by de Wolff (1974). There exists a three-dimensional reciprocal unit cell, for only the main reflections, defined by  $\mathbf{a}^*$ ,  $\mathbf{b}^*$  and  $\mathbf{c}^*$ . The relationship between the above two reciprocal unit cells is given by

$$\mathbf{b}_1 = \mathbf{a}^*, \quad \mathbf{b}_2 = \mathbf{b}^*, \quad \mathbf{b}_3 = \mathbf{c}^* \quad \text{and} \quad \mathbf{b}_4 = k\mathbf{c}^* + \mathbf{d},$$

while the two corresponding direct cells are related to each other by

$$\mathbf{a}_1 = \mathbf{a}, \quad \mathbf{a}_2 = \mathbf{b}, \quad \mathbf{a}_3 = \mathbf{c} - k\mathbf{d} \quad \text{and} \quad \mathbf{a}_4 = \mathbf{d},$$

where  $a = b = 10.12$ ,  $c = 2.96 \text{ \AA}$ ,  $k = 1/2.27$  and  $\mathbf{d}$  is a unit vector perpendicular to the three-dimensional physical space. Only the intensities of reflections up to about  $0.9 \text{ \AA}$  resolution on the  $h0l$  reciprocal plane have been measured. In order to increase the accuracy of the intensity measurement, five photographs were taken for the same diffraction pattern with different exposure times. This is an analogue of the multiple-film technique for recording X-ray diffraction intensities by photographic methods. The photographs were measured using a Perkin Elmer PDS microdensitometer data acquisition system with a  $50 \times 50 \mu\text{m}$  aperture. The diffraction pattern was divided into 512 pixels along  $\mathbf{a}^*$  from  $-h_{\text{max}}$  to  $+h_{\text{max}}$  and divided into 231 pixels along  $\mathbf{c}^*$  from 0 to  $l_{\text{max}}$ . The integrated intensity of each reflection was obtained by summing up the density  $D = \ln(I_0/I)$  on the pixels within the diffraction spot and then subtracting the background. The intensities of symmetrically equivalent reflections were averaged. Structure-factor amplitudes were obtained from the square roots of integrated diffraction intensity. The  $R$  factor with

Table 1. Structure factors of the main reflections

$$\mathbf{H} = h_1\mathbf{b}_1 + h_2\mathbf{b}_2 + h_3\mathbf{b}_3 + h_4\mathbf{b}_4.$$

$h_1$	$h_2$	$h_3$	$h_4$	$ F_o(\mathbf{H}) $	$ F_c(\mathbf{H}) $	Sign*
0	0	0	0	20.40	116.46	+
0	0	2	0	9.41	25.28	+
1	0	1	0	14.78	7.73	-
1	0	3	0	2.49	1.85	-
2	0	0	0	13.87	14.03	-
2	0	2	0	4.82	3.75	-
3	0	1	0	15.16	15.96	-
3	0	3	0	2.39	3.69	-
4	0	0	0	13.28	14.54	-
4	0	2	0	3.96	4.65	-
5	0	1	0	8.48	7.95	+
5	0	3	0	1.09	1.12	+
6	0	0	0	10.62	11.64	+
6	0	2	0	5.54	5.98	+
7	0	1	0	4.62	1.64	-
7	0	3	0	1.39	1.07	-
8	0	0	0	5.00	4.64	+
8	0	2	0	2.12	2.81	+
9	0	1	0	4.50	5.32	-
9	0	3	0	1.00	2.17	-
10	0	0	0	3.19	2.88	-
10	0	2	0	1.86	1.23	-
11	0	1	0	1.49	0.20	+
12	0	0	0	2.22	1.97	+

\* Signs were calculated from the refined average structure.

Table 2. Structure factors of the satellite reflections

$$\mathbf{H} = h_1\mathbf{b}_1 + h_2\mathbf{b}_2 + h_3\mathbf{b}_3 + h_4\mathbf{b}_4.$$

$h_1$	$h_2$	$h_3$	$h_4$	$ F_o(\mathbf{H}) $	$F_c(\mathbf{H})$	Sign*
0	0	2	-2	2.04	1.48	+
1	0	1	-2	2.49	-3.21	-
2	0	2	-2	1.99	1.32	+
3	0	1	-2	1.98	-1.77	-
4	0	2	-2	0.95	1.02	+
5	0	1	-2	1.07	-1.12	-
6	0	2	-2	0.57	0.76	+
0	0	2	-1	2.35	-2.47	-
1	0	1	-1	5.14	5.08	+
1	0	3	-1	0.74	1.38	+
2	0	2	-1	2.20	-2.30	-
3	0	1	-1	4.33	3.44	+
3	0	3	-1	0.59	1.28	+
4	0	2	-1	1.59	-1.92	-
5	0	1	-1	2.68	2.32	+
6	0	2	-1	1.11	-1.51	-
7	0	1	-1	1.41	1.63	+
8	0	2	-1	0.76	-1.15	-
9	0	1	-1	1.05	1.16	+
0	0	0	1	5.98	-5.83	-
0	0	2	1	0.63	-1.06	-
1	0	1	1	2.38	2.12	+
2	0	0	1	5.36	-4.24	-
2	0	2	1	0.58	-1.02	-
3	0	1	1	1.97	1.83	+
4	0	0	1	3.28	-2.70	-
4	0	2	1	0.51	-0.91	-
5	0	1	1	1.16	1.45	+
6	0	0	1	1.84	-1.83	-
7	0	1	1	0.95	1.11	+
8	0	0	1	1.10	-1.29	-
0	0	0	2	2.77	1.81	+
1	0	1	2	0.81	-0.90	-
2	0	0	2	1.94	1.56	+
4	0	0	2	0.92	1.14	+
6	0	0	2	0.72	0.82	+

\* Signs were derived by direct method.

respect to the discrepancy of symmetrically equivalent reflections is 0.115, which was calculated according to the following expression:

$$R = \frac{\sum_H \|F(H)\| - \langle |F(H)| \rangle}{\sum_H \langle |F(H)| \rangle},$$

where  $|F(H)|$  is a structure-factor amplitude before averaging, while  $\langle |F(H)| \rangle$  is the corresponding average value of the symmetrically equivalent reflections. As shown in Tables 1 and 2, there are in total 60 independent  $h0l$  reflections including 24 main and 36 satellite reflections.

### Average structure

According to Zhou & Ma (1987), ankangite is isomorphous with hollandite (Byström & Byström, 1950), as far as the average structure is concerned. The space group of hollandite is  $I4/m$ . A projection of the structure of hollandite along the  $c$  axis is shown in Fig. 1, where the Mn atoms should be replaced by Ti for ankangite. *Ab initio* determination of the average structure of ankangite is difficult using only the  $h0l$  reflections because the atoms overlap greatly on the projection along the  $b$  axis. We started from the model of hollandite, which yielded an initial  $R$  factor of 0.59 for the 23 main reflections [not including  $F(000)$ ]. Refinement of the average structure was carried out first by a parameter-shift method assuming the space group  $I4/m$ , *i.e.* to keep all atoms lying on the mirror plane perpendicular to the  $c$  axis. This resulted in an  $R$  factor of 0.278. After that, a refinement was tried to move the atoms away from the mirror plane of  $I4/m$  by lowering the space-group symmetry to  $I4$ . However, no observable shift of

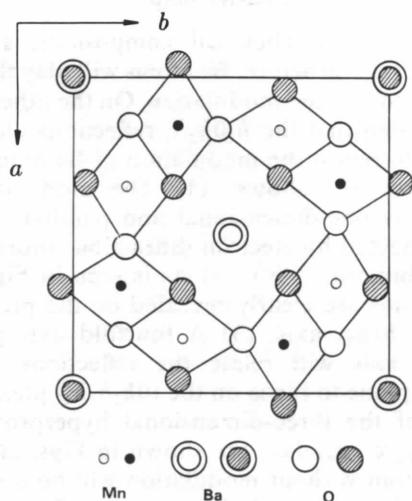


Fig. 1. The structure diagram of hollandite according to Byström & Byström (1950). Open circles are at level  $z=0$ ; filled circles are at level  $z=\frac{1}{2}$ .

Table 3. Atomic parameters of ankangite and hollandite

$B$  = temperature factor ( $\text{\AA}^2$ );  $Q$  = occupancy.

#### (a) Average structure of ankangite

	$x$	$y$	$z$	$B$	$Q$
Ba	0.000	0.000	0.500	0.50 (41)	0.4
Ti	0.366 (3)	0.155 (3)	0.000	2.50 (27)	1.0
O1	0.165 (8)	0.198 (8)	0.000	3.00 (61)	1.0
O2	0.572 (8)	0.248 (11)	0.000	3.75 (78)	1.0

#### (b) Hollandite (Byström & Byström, 1950).

	$x$	$y$	$z$
Ba	0.000	0.000	0.500
Mn	0.348	0.167	0.000
O1	0.153	0.180	0.000
O2	0.542	0.167	0.000

atomic positions along the  $c$  axis or improvement on the  $R$  factor was found. This confirms the space-group symmetry of  $I4/m$  for the average structure. The corresponding calculated structure factors are listed in Table 1. Atomic parameters obtained after refinement are listed in Table 3. A projection of the electron potential distribution along the  $b$  axis of the average structure is shown in Fig. 2(a). It is seen from

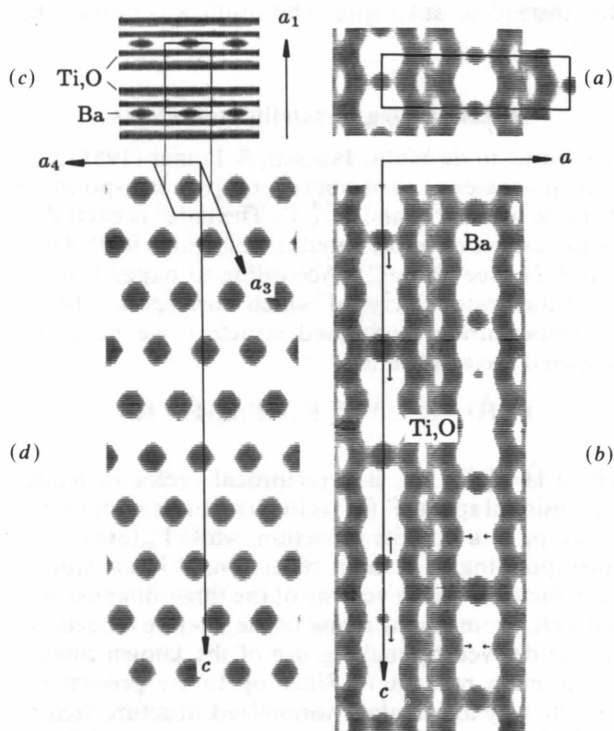


Fig. 2. Fourier maps of ankangite. (a)  $\varphi(x, z)_{AV}$ , projection of the average structure along the  $b$  axis, a unit cell of which is shown as the rectangle; (b)  $\varphi(x, z)_{IN}$ , projection of the incommensurate modulated structure along the  $b$  axis; (c)  $\int_0^1 \varphi(x_1, x_2, \frac{1}{2}, x_4) dx_2$ , a unit cell of which is shown as the rectangle; (d)  $\int_0^1 \varphi(0, x_2, x_3, x_4) dx_2$ , a unit cell of which is shown as the parallelogram.

Table 1 that the calculated structure-factor magnitudes of (0000) and (0020) are much greater than those of the observed ones. This indicates strong dynamic diffraction effects. On the other hand, the calculated magnitude of 1010 is much smaller than the observed one. This can be explained by the superposition of some secondary reflections onto 1010. The secondary reflections  $10\bar{1}0$  and 1030, produced by using 0020 and 0020 as incident beam, respectively, coincide and are in phase with the primary reflection 1010. The  $R$  factor calculated for the main reflections excluding the above three reflections is 0.153. Comparing the atomic positions of ankangite with hollandite, we found that there is no great change in positions of the heavy atoms. However, the O atoms adjacent to Ba on the same  $z$  level shift towards the Ba sites resulting in some abnormal interatomic distances. This can easily be explained by the vacancy on Ba sites found later. The relatively high temperature factors for Ti and O atoms indicate the possibility of positional modulation. Despite the comparatively large shifts of some atomic parameters, most signs of the main reflections remained unchanged during the refinement. In the test on deriving signs for the satellite reflections, we tried to start with signs of main reflections calculated from hollandite instead of ankangite. The result was almost the same.

### Direct phasing of satellite reflections

According to de Wolff, Janssen, & Janner (1981), the four-dimensional superspace groups corresponding to  $I4/m$  are  $P_{1\bar{1}}^{I4/m}$  and  $P_{S\bar{1}}^{I4/m}$ . The latter is excluded by the existence of the satellite reflections 0001, 0021 and 002 $\bar{1}$  (see Table 2). According to paper I, for a multi-dimensional crystal which corresponds to an incommensurate modulated structure we have the modified Sayre equation:

$$F_s(\hat{\mathbf{H}}) = (2\theta/V) \sum_{\hat{\mathbf{H}}'} F_m(\hat{\mathbf{H}}') F_s(\hat{\mathbf{H}} - \hat{\mathbf{H}}'), \quad (1)$$

where  $\hat{\mathbf{H}} = \sum_{i=1}^{3+n} h_i \mathbf{b}_i$  is a reciprocal vector in multi-dimensional space,  $F_s(\hat{\mathbf{H}})$  is the structure factor corresponding to a satellite reflection, while  $F_m(\hat{\mathbf{H}})$  is that corresponding to a main reflection,  $\theta$  is an atomic form factor,  $V$  is the volume of the three-dimensional unit cell. From (1) the phase of the satellite reflections can be derived by making use of the known phases of the main reflections. Since up to the present we have no way to calculate normalized structure factors  $E(\hat{\mathbf{H}})$  for an unknown incommensurate modulated structure, we use  $F(\hat{\mathbf{H}})$  instead of  $E(\hat{\mathbf{H}})$  throughout the following phase derivation process. A starting set consisting of 34 reflections was used, which includes the total 24 main reflections with known signs and 10 satellite reflections, selected by a convergence procedure, with signs assigned by a random-number

generator. Fifty random trials were performed. The residual figure of merit defined as the following was used to evaluate the results.

$$R_\alpha = \sum_{\hat{\mathbf{H}}} |\alpha_{\text{est}} - \alpha| / \sum_{\hat{\mathbf{H}}} \alpha_{\text{est}},$$

where

$$\alpha^2 = \left[ \sum_{\hat{\mathbf{H}}'} \kappa \cos \Phi \right]^2 + \left[ \sum_{\hat{\mathbf{H}}'} \kappa \sin \Phi \right]^2,$$

$$\alpha_{\text{est}} \sim \sum_{\hat{\mathbf{H}}'} \kappa I_1(\kappa) / I_0(\kappa),$$

$$\kappa = 2\sigma_3 \sigma_2^{-3/2} |F(\hat{\mathbf{H}}) F(\hat{\mathbf{H}}') F(\hat{\mathbf{H}} - \hat{\mathbf{H}}')|,$$

$$\Phi = \varphi_{\hat{\mathbf{H}}} + \varphi_{\hat{\mathbf{H}} - \hat{\mathbf{H}}'}.$$

The above definition is similar to that used in the program *MULTAN* (Main, Fiske, Hull, Lessinger, Germain, Declercq & Woolfson, 1980). Of the 50 random trials, 5 having the smallest  $R_\alpha$ 's correspond to the same set of resulting signs listed in Table 2. An inverse Fourier transform was then calculated using the  $F_{\text{obs}}$  and signs listed in Tables 1 and 2. The result is a four-dimensional electron potential distribution projected along the  $a_2$  axis onto a three-dimensional hyperplane, i.e.  $\int_0^1 \varphi(x_1, x_2, x_3, x_4) dx_2$ . By cutting this hyperprojection perpendicular to  $\mathbf{a}_4$  we obtained the projection of the incommensurate modulated structure along the  $b$  axis,  $\varphi(x, z)_{1N}$  in Fig. 2(b), which reveals the form of modulation in the real physical space without relying on preliminary assumptions. In order to obtain more-accurate information of the modulation, a quantitative analysis of the hyperprojection is necessary.

### Modulation of Ba atoms determined directly from the Fourier map

According to the chemical composition and the known average structure, Ba atoms will play the most important role in the modulation. On the other hand, we concluded that the  $h_1 0 h_3 h_4$  reflections alone are sufficient to reveal the modulation of Ba atoms. The reasons are as follows: (1) The modulation in ankangite is one-dimensional and parallel to the  $c$  axis as detected by electron diffraction studies (Wu, Li & Hashimoto, 1990). (2) As is seen in Fig. 2(a), the Ba atoms are clearly revealed on the projection along the  $b(a_2)$  axis. (3) A fourfold axis parallel to the  $c$  axis will relate the reflections on the  $(h_1 0 h_3 h_4)$  plane to those on the  $(0 h_2 h_3 h_4)$  plane. Two sections of the three-dimensional hyperprojection,  $\int_0^1 \varphi(x_1, x_2, x_3, x_4) dx_2$ , are shown in Figs. 2(c) and (d). An atom without modulation will be a straight bar parallel to the fourth dimension  $\mathbf{a}_4$ . Occupational modulation causes a periodic variation on the width, while positional modulation causes a periodic variation on the direction of the bar. In Figs. 2(c) and

(d) very strong occupational modulation of Ba atoms is seen. In addition, positional modulation can also be observed as indicated by the short arrows in Fig. 2(b).

According to formula (9) of paper I, a modulated structure can be expressed in terms of modulated atoms situated on their average positions in three-dimensional space with atomic scattering factors given by (8) of paper I. In the case of ankangite, the structure-factor formula for satellite reflections, neglecting the contribution from the modulation of Ti and O atoms will be

$$F(\hat{\mathbf{H}}) = 2f_{\text{Ba}}(\hat{\mathbf{H}}) \cos(\pi h_3) \quad (2)$$

and the modulated atomic scattering factor for Ba, with respect to an origin at its average position (0, 0, 1/2, 0), becomes

$$f_{\text{Ba}}(\hat{\mathbf{H}}) = f_{\text{Ba}}(\mathbf{H}) \int_0^1 P(\bar{x}_4) \times \cos\{2\pi[(h_3 + kh_4)U_3(\bar{x}_4) + h_4\bar{x}_4]\} d\bar{x}_4, \quad (3)$$

where  $f_{\text{Ba}}(\mathbf{H})$  is the normal atomic scattering factor multiplied by the temperature factor  $\exp(-B|\mathbf{H}|^2/4)$ .  $U_3(\bar{x}_4)$  is the positional modulation function, which describes the deviation of Ba from its average position as a function of  $\bar{x}_4$ .  $P(\bar{x}_4)$  is the occupational modulation function, which describes the variation of the occupancy of Ba as a function of  $\bar{x}_4$ . Since  $U_3(\bar{x}_4)$  is defined in the region with  $x_4$  ranging from 0 to 1, where  $x_4 = \bar{x}_4 + kU_3(\bar{x}_4)$  (see Fig. 3), in order to determine the positional modulation function  $U_3(\bar{x}_4)$  from the Fourier map, only a part of Fig. 2(d) is needed. This is shown in Fig. 4(a). The electron potential distribution in Fig. 4(a) was sampled by 65 lines parallel to the  $a_3$  axis and equally spaced in the range from  $x_4 = 0$  to  $x_4 = 1$ . The position of the maximum electron potential on a line yields approximately the value of  $U_3(\bar{x}_4)$  corresponding to a particular  $\bar{x}_4$ . The form of  $U_3(\bar{x}_4)$  so obtained is shown graphically in Fig. 4(b) revealing clearly the positional modulation of the Ba atoms. For obtaining approximately the occupational modulation function  $P(\bar{x}_4)$ , the values

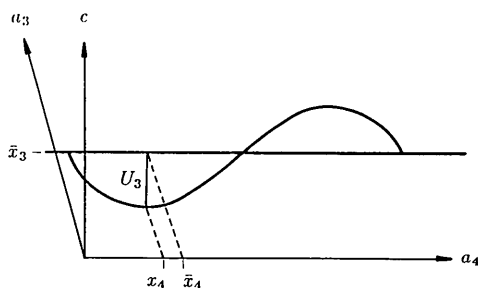


Fig. 3. The relationship between  $x_4$  and  $\bar{x}_4$ .

of the electron potential along the curve in Fig. 4(b) was drawn against  $\bar{x}_4$ . The result is shown in Fig. 4(c). With the values of  $U_3(\bar{x}_4)$  and  $P(\bar{x}_4)$  corresponding to Figs. 4(b) and (c)  $R$  factors were calculated for the first and second order of satellite reflections giving the values of 0.192 and 0.366, respectively. Since both the curves in Figs. 4(b) and (c) were obtained from the Fourier map, they are not independent of each other and they suffer from errors due to the truncation of the Fourier series and the dynamic electron diffraction effect of the main reflections. Nevertheless, the shape of  $U_3(\bar{x}_4)$  suggested that it can be described by the following analytic expression:

$$U_e(\bar{x}_4) = D_1 \sin 2\pi(\bar{x}_4 - \frac{1}{2}) + D_2[\sin 2\pi(\bar{x}_4 - \frac{1}{2})]^3 + D_3[\sin 2\pi(\bar{x}_4 - \frac{1}{2})]^5. \quad (4)$$

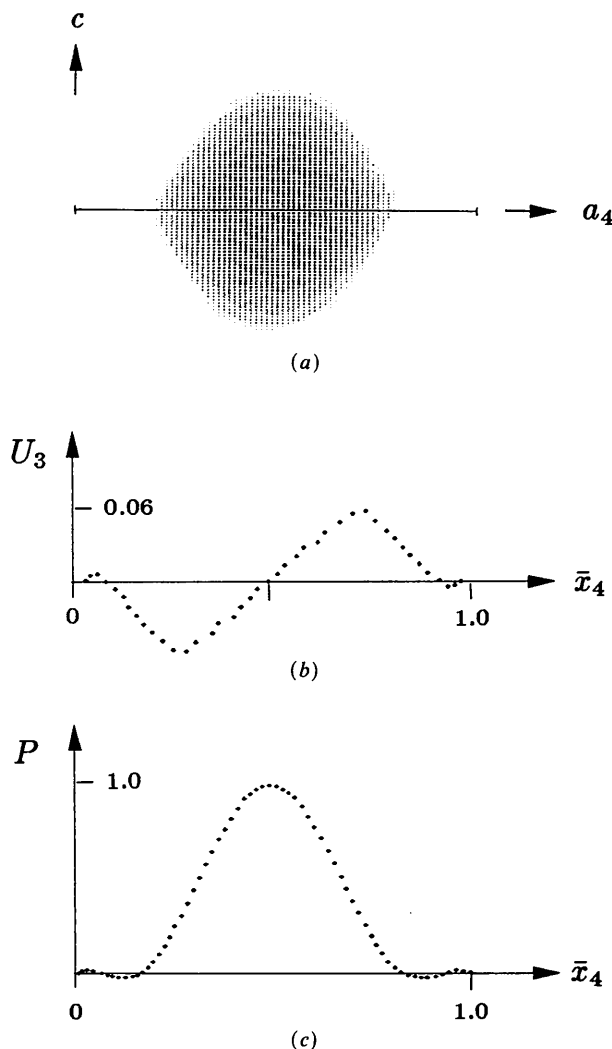


Fig. 4. Determination of the modulation functions for Ba atoms. (a) Electron potential distribution of Ba from  $x_4 = 0$  to  $x_4 = 1$ ; (b) positional modulation function of Ba from  $\bar{x}_4 = 0$  to  $\bar{x}_4 = 1$ ; (c) occupational modulation function of Ba from  $\bar{x}_4 = 0$  to  $\bar{x}_4 = 1$ .

Table 4. *Parameters in the analytic expressions (4) and (5)*

$A_1$	-3.49 (2)	$C$	0.123 (14)
$A_2$	4.33 (2)	$D_1$	-0.042 (3)
$B_1$	96.6 (84)	$D_2$	0.077 (4)
$B_2$	71.5 (49)	$D_3$	0.021 (2)

Table 5. *R factors for different reflection subsets*

Total reflections*	Main reflections*	Satellite reflexions		
		Total	First order	Second order
0.190	0.153	0.187	0.176	0.234

\* Not including the reflections 0000, 0020 and 1010.

On the other hand, the shape of  $P(\bar{x}_4)$  suggested the expression

$$P(\bar{x}_4) = A_1 \exp \left[ -B_1 \left( \bar{x}_4 - \frac{1}{2} \right)^2 \right] + A_2 \exp \left[ -B_2 \left( \bar{x}_4 - \frac{1}{2} \right)^2 \right] + C. \quad (5)$$

All the adjustable parameters in (4) and (5) are listed in Table 4. They were determined by a parameter-shift procedure which minimizes the following  $R$  factor:

$$R = \sum_{\bar{h}} \frac{||F_o| - |F_c||}{\sum_{\bar{h}} |F_o|}.$$

Here  $F_o$  and  $F_c$  denote, respectively, the observed and calculated structure factors for the satellite reflections. They are listed in Table 2. Final  $R$  factors for the total and subset reflections are listed in Table 5. Values of the  $R$  factors, although relatively high, are still reasonable in view of the fact that the measurement of diffraction intensity for electrons cannot be as accurate as for X-rays and that the modulation of Ti and O atoms have not been considered.

### Discussion

Modulation of Ti and O atoms can also be found by a careful inspection of Figs 2(b) and (c). However, since atoms of Ti and O overlap and the modulations are much weaker than that of Ba atoms, it is difficult to determine the modulation functions quantitatively.

Comparison of Figs. 2(b) and (d) shows that the modulation of Ba along the  $a_4$  axis causes mainly

two effects in the three-dimensional physical space: (1) vacancies of Ba are ordered parallel to the  $c$  axis with a period 2.27 times longer than  $c$ . This gives rise to the sharp satellite reflections; (2) as shown in Fig. 2(b), the occupancy of Ba atoms varies between 0 and 1. This implies that the vacancies of Ba are disordered perpendicular to the  $c$  axis. Consequently, continuous diffuse scattering should appear on the reciprocal planes containing the satellite reflections and parallel to the  $a^*b^*$  plane. This has already been observed by Wu, Li & Hashimoto (1990).

Solving an incommensurate modulated structure by electron diffraction analysis although giving less-accurate results than with X-ray analysis offers the advantage that there is no need to prepare good-quality single crystals of sufficient size. This is particularly important since good-quality single crystals are often difficult to grow for many incommensurate modulated phases.

The direct method has proved very successful even with poor-quality data. Without making any assumption, it revealed intuitively the modulation function of the Ba atoms as shown in Figs. 4(b) and (c), which otherwise would be very difficult to predict.

The authors thank the referees, their comments have improved the manuscript. One of us (LFH) is indebted to Professor Ma Zhe-sheng for providing the mineral specimen of ankangite.

### References

- BYSTRÖM, A. & BYSTRÖM, A. M. (1950). *Acta Cryst.* **3**, 146-154.  
 HAO, Q., LIU, Y.-W. & FAN, H.-F. (1987). *Acta Cryst.* **A43**, 820-824.  
 MAIN, P., FISKE, S. J., HULL, S. E., LESSINGER, L., GERMAIN, G., DECLERCQ, J.-P. & WOOLFSON, M. M. (1980). *MULTAN80. A System of Computer Programs for the Automatic Solution of Crystal Structures from X-ray Diffraction Data*. Univ. of York, England, and Louvain, Belgium.  
 WOLFF, P. M. DE (1974). *Acta Cryst.* **A30**, 777-785.  
 WOLFF, P. M. DE, JANSSEN, T. & JANNER, A. (1981). *Acta Cryst.* **A37**, 625-636.  
 WU, X.-J., LI, F.-H. & HASHIMOTO, H. (1990). *Acta Cryst.* **B46**, 111-117.  
 XONG, M., MA, Z.-S. & PENG, Z.-Z. (1984). A Report to the International Mineral Commission.  
 ZHOU, J. & MA, Z.-S. (1987). *Geoscience*, **1**, 77-83. (In Chinese.)